

Radix Stellariae extract prevents high-fat-diet-induced obesity in C57BL/6 mice by accelerating energy metabolism

Yin Li ¹, Xin Liu ¹, Yu Fan ¹, Baican Yang ^{Corresp.}, ¹, Cheng Huang ^{Corresp.}, ¹

¹ School of Pharmacy, Shanghai University of Traditional Chinese Medicine, Shanghai, China

Corresponding Authors: Baican Yang, Cheng Huang
Email address: bcy2002@sina.com, chuang@shutcm.edu.cn

Stellaria dichotoma L., is widely distributed in Ningxia and surrounding areas in northwestern China. Its root, Radix Stellariae (RS), has been used in herbal formulae for treating asthenic-fever, infection, malaria, dyspepsia in children and several other symptoms. This study investigated whether the RS extract (RSE) alleviates metabolic disorders. The results indicated that RSE significantly inhibited body weight gain in high-fat (HF)-diet-fed C57BL/6 mice, reduced fasting glucose levels, and improved insulin tolerance. Moreover, RSE increased the body temperature of the mice and the expression of uncoupling proteins and peroxisome proliferator-activated receptors in the white adipose tissue. Thus, RSE alleviated metabolic disorders in HF-diet-fed C57BL/6 mice by potentially activating UCP and PPAR signaling.

1 **Radix Stellariae extract prevents high-fat-diet-induced obesity in**
2 **C57BL/6 mice by accelerating energy metabolism**

3 Yin Li, Xin Liu, Yu Fan, Baican Yang*, Cheng Huang*

4 *School of Pharmacy, Shanghai University of Traditional Chinese Medicine, 1200 Cailun Road,*
5 *Shanghai 201203, China*

6

7 ** Corresponding author:*

8 1. *Cheng Huang, Drug Discovery Lab, School of Pharmacy, Shanghai University of Traditional*
9 *Chinese Medicine, 1200 Cailun Road, Shanghai 201203, China (chuang@shutcm.edu.cn). Tel:*
10 *+86-21-51322182; fax: +86-21-51322193.*

11 2. *Baican Yang, School of Pharmacy, Shanghai University of Traditional Chinese Medicine,*
12 *1200 Cailun Road, Shanghai 201203, China (bcy2002@sina.com).*

13

14

15

16

17

18

19

20

21

22

23

24

25

26

27

28

29

30

31

32

33

34

35

36

37

38

39

40

41 **ABSTRACT**

42

43 *Stellaria dichotoma L.*, is widely distributed in Ningxia and surrounding areas in northwestern
44 China. Its root, Radix Stellariae (RS), has been used in herbal formulae for treating asthenic-
45 fever, infection, malaria, dyspepsia in children and several other symptoms. This study
46 investigated whether the RS extract (RSE) alleviates metabolic disorders. The results indicated
47 that RSE significantly inhibited body weight gain in high-fat (HF)-diet-fed C57BL/6 mice,
48 reduced fasting glucose levels, and improved insulin tolerance. Moreover, RSE increased the
49 body temperature of the mice and the expression of uncoupling proteins and peroxisome
50 proliferator-activated receptors in the white adipose tissue. Thus, RSE alleviated metabolic
51 disorders in HF-diet-fed C57BL/6 mice by potentially activating UCP and PPAR signaling.

52

53 **INTRODUCTION**

54

55 Metabolic syndrome (MS) is prevalent world-wide, particularly in Western countries. It is
56 characterized by obesity, insulin resistance, hyperlipidemia, type 2 diabetes mellitus,
57 hypertension, and atherosclerotic cardiovascular disease (*Morikawa et al., 2004; Eckel et al.,*
58 *2010*). Excessive calorie intake and lack of exercise are the two main reasons leading to MS.
59 Recent relevant experimental and clinical research results can be summarized as follows: (1)
60 develop practical methods to address the main causes of MS, and (2) identify a direct method to
61 eliminate adverse factors, such as insulin resistance, hyperlipidemia, obesity, and hypertension
62 (*Ginsberg, 2003*). Thus, although difficult, novel therapeutics to prevent and treat obesity are
63 urgently required (*Apovian et al., 2015*).

64

65 Brown adipose tissue (BAT) is essential for thermogenesis and body temperature maintenance
66 (*Harms & Seale, 2013*). When activated, BAT can express uncoupling protein1(UCP1) to release
67 energy in the form of heat by uncoupling the protons generated by substrate oxidation during
68 adenosine triphosphate (ATP) production (*Izzi-Engbeaya et al., 2015*). Moreover, white adipose
69 tissue (WAT) can be used as an index of energy metabolism for its browning. UCP1, UCP2, and
70 UCP3 are related to energy metabolism; in particular UCP1 plays a critical role in releasing
71 electrons rather than storing them, resulting in heat release (*Kim & Plutzky, 2016*).

72

73 Peroxisome proliferator-activated receptors (PPARs) are members of the nuclear receptor
74 family (*Francis et al., 2003*). PPAR α , PPAR β , and PPAR γ are their three isoforms. PPARs are
75 crucial regulators of lipid, glucose and tissue metabolism as well as cell differentiation and
76 proliferation, apoptosis, and host immunity (*Desvergne & Wahli, 1999*). PPARs bind to the
77 retinoid X receptors to form heterodimers, which regulate downstream gene expression by
78 interacting with PPAR response elements in these genes (*Wahli, Braissant & Desvergne, 1995*).

79 PPAR α is present in the liver (*Jia et al., 2003*), heart (*Barger & Kelly, 2000; Gilde & Van Bilsen,*
80 *2003*), skeletal muscle, BAT and kidneys. It mainly mediates the uptake and β -oxidation of fatty
81 acids in the liver and heart (*Bishop-Bailey, 2000; Puddu, Puddu & Muscari, 2003*). The
82 activation of PPAR α is an effective therapy for hyperglyceridemia. PPAR γ is expressed
83 abundantly in adipocytes, particularly in WAT, as well as in the gastrointestinal tract and
84 macrophages (*Thompson, 2007*). It plays a key role in adipocyte differentiation, lipid
85 accumulation, and insulin sensitivity (*Spiegelman, 1998; Francis et al., 2003*), and is involved in
86 whole-body glucose homeostasis (*Barroso et al., 1999*). As we all known, PPAR γ is the target of
87 the insulin-sensitizing agent rosiglitazone.

88

89 Radix Stellariae (RS), also called Yinchaihu, the root of *Stellaria dichotoma*, a common
90 Chinese herbal medicine used clinically to treat fever and infantile malnutrition. RS was first
91 described in “Ben Cao Gang Mu” 400 years ago (*Teng, 1985*). According to the clinical studies,
92 RS also has several other pharmacological functions, including anti-inflammatory (*Chen et al.,*
93 *2010*), anti-cancer, and anti-allergic activities (*Morikawa et al., 2004; Sun et al., 2004*) as well as
94 dilation of blood vessels (*Morita et al., 2005*). Recently, it has been reported that RS had a
95 higher content of α -spinasterol, which has anti-inflammatory and antipyretic effect and β -
96 carboline alkaloids in RSE with anti-allergy properties through the mice anti-allergic reaction
97 experiment (*Morikawa et al., 2004*). Besides, new cyclicpeptids extracted from RS has been
98 demonstrated with antitumor activity in vitro and mild dilation of blood vessels. Nevertheless,
99 the effects of RS on metabolic disorders have not been reported.

100 In this study, we observed the effects of RSE on HF-diet-induced obesity to assay whether RS
101 could alleviate metabolic disorders. We found that it can alleviate MS by reducing body weight
102 and blood glucose levels, increasing insulin sensitivity in HF-diet-induced obese mice.

103

104 MATERIALS AND METHODS

105

106 Preparation of Radix Stellariae extract

107

108 RS was purchased from the Ningxia province. In a spherical extractor, 4L of 95% ethanol was
109 added to 500g of RS. Extraction was performed for 2 h at 85°C, followed by cooling and
110 filtering of the extract. Extraction was repeated using 50% ethanol. The extracted solutions were
111 combined for rotatory evaporation at 60°C, under reduced pressure, till the taste of alcohol was
112 undetectable. Finally, the concentrated solution was freeze-dried and stored at -20°C.

113

114 Liquid chromatograph-high resolution mass spectrometry

115

116 Liquid chromatography-high resolution mass spectrometry (LC-HRMS) was performed using a
117 Waters ACQUITY UPLC system, equipped with a binary solvent delivery manager and a sample
118 manager. This system was, coupled with a Waters Micromass Q-TOF Premier Mass
119 Spectrometer, equipped with an electrospray interface (Waters Corporation, Milford, MA).

120

121 An Acquity BEH C18 column (100 mm × 2.1 mm; i.d., 1.7 μm; Waters, Milford, USA) was
122 maintained at 50 °C and eluted with gradient solvent from A : B (95 : 5) to A : B (0 : 100) at a
123 flow rate of 0.40 mL/min, where A is aqueous formic acid (0.1% (v/v) formic acid) and B is
124 acetonitrile (0.1% (v/v) formic acid) with an injection volume of 5.0 μL. The following gradient
125 was applied (0 - 4.00 min: 95.0% A + 5.0% B; 4.00 - 6.00min: 80.0% A + 20.0% B; 6.00 - 8.00
126 min: 75.0% A + 25.0% B; 8 - 12.5 min: 50.0% A + 50.0% B; 12.5 - 13.5 min: 15.0% A + 85.0%
127 B; 13.5 - 15 min: 0.0% A + 100.0% B).

128

129 The MS analyses were performed using positive and negative ions channels. The ionization
130 conditions were optimized, and the operating parameters were as follows: Polarity: positive/
131 negative; Capillary voltage: 3.0 kV/2.8 kV; Sampling cone: 35 V/45 V; Collision energy: 3 eV/3
132 eV; Source temperature: 115°C/115°C; Desolvation temperature: 350°C/350°C; Desolvation gas:
133 600 L/hr/ 600 L/hr; Scan range: m/z 50 -1500/ m/z 50 - 1500; Scan time: 0.3 s/0.3 s; Interscan
134 time: 0.02 s/0.02 s.

135

136 **Animals and diets**

137

138 Six-week-old female C57BL/6 mice were purchased from the SLAC Laboratory (Shanghai,
139 China). The animal protocols used in this study were approved by the Shanghai University of
140 Traditional Chinese Medicine (approval number 2014019). The mice were housed under 22°C -
141 23°C with a 12 h light/dark cycle. After a 1 week adaptation period, we randomly divided the
142 seven-week-old mice into three groups. They were fed a chow diet (Chow, 10% of calories
143 derived from fat, Research Diets; D12450B), an HF diet (HF, 60% of calories derived from fat,
144 Research Diets; D12492), or a diet supplemented with 1% RSE (HF + RSE). The mice had free
145 access to food and water for 8 weeks. We weighed the food intake and body weight every 2 days.

146

147 **Rectal temperature measurement**

148

149 At the end of 8 weeks, the rectal temperature of the mice was recorded three times at 3 PM by
150 using an instrument for measuring rectal temperature, at intervals of 2 days.

151

152 **Intraperitoneal glucose tolerance test**

153

154 All mice were fasted for 12 h overnight at the end of the preventive experiment. For the
155 intraperitoneal glucose tolerance test (IPGTT), we collected the blood samples from the tail vein
156 for determination of baseline glucose values (0 min). Next intraperitoneal injections of glucose
157 (1 g/kg body weight) were administered to all the mice in 15 min, and blood glucose levels were
158 measured at regular intervals (15, 30, 60, and 90 min) after the injection of glucose.

159

160 **Intraperitoneal insulin tolerance test**

161

162 The mice were not fasted for the intraperitoneal insulin tolerance test (IPITT). Similar to the
163 IPGTT, the basal blood glucose levels (0 min) were measured from the tail vein before the
164 injection of insulin (0.75 U/kg body weight). The insulin was diluted in physiological saline.
165 Next, additional blood glucose levels were measured at 15, 30, 60, 90, and 120 min after the
166 injection of insulin.

167

168 **Serum chemistry analysis**

169

170 The mice were fasted for 10 h overnight at the end of the animal preventive experiment; the next
171 day, all mice were anesthetized using 20% urethane before sample and tissue collection. Blood
172 samples were drawn from the heart using a 1mL syringe. After clotting at room temperature for
173 over 2 h, the serum was separated from the blood samples. After centrifugation, 120 μ L of serum
174 was drawn from every sample, and the serum total cholesterol (TC), triglyceride (TG), low-
175 density lipoprotein cholesterol (LDL-c), high-density lipoprotein cholesterol (HDL-c), alanine
176 aminotransferase (ALT) and aspartate aminotransferase (AST) levels were analyzed using a
177 Hitachi 7020 Automatic Analyzer.

178

179 **Morphological analysis of white adipose tissue**

180

181 To examine the structure of WAT, the WAT samples were fixed in 4% paraformaldehyde. The
182 tissue samples were sectioned at 5 μ m intervals and stained with Hematoxylin and Eosin (H &
183 E). The stained samples were examined under a light microscope.

184

185 **Reporter assay**

186

187 The reporter assay has been performed using the Dual-Luciferase Reporter Assay System
188 (Promega, USA) as previously described. The expression plasmids for pCMXGal-hPPAR α , β , γ
189 and the Gal4 reporter vector MH100 \times 4-TK-Luc were co-transfected with a reporter construct
190 so that 1 μ g of the relevant plasmid combined with 1 μ g of reporter plasmids and 0.1 μ g of pREP7
191 (*Renilla luciferase*) reporter could be used to normalize transfection efficiencies. The
192 transfection mixture, which contained 10 μ g of total plasmids and 15 μ l FuGENE[®]HD per ml of
193 DMEM, was added to HEK293T cells for 24 h and then removed. The PPAR α , β , γ agonists
194 (Fenofibric acid, GW7647, Pioglitazone) and 2.5, 5, 10, 20, 50, 100, 200, 400, 600, 800, 1000 μ g
195 /ml of RSE were added to fresh media and the cells were incubated for another 24 h to determine
196 luciferase activity.

197

198 **Quantitative real-time polymerase chain reaction (Real time qPCR)**

199

200 The total RNA of WAT and BAT was extracted using the RNAiso Plus (Takara, Dalian, China).
201 RNA is unstable, and to facilitate stable long-term preservation, we used the RevertAid First

202 Strand cDNA Synthesis Kit (Thermo Scientific, Wilmington, Delaware, USA) for the first-strand
203 cDNA (42°C, 1h; 70°C, 5min). The gene expression levels were analyzed using quantitative
204 real-time RT-PCR conducted using the ABI StepOnePlus real-time PCR system (Applied
205 Biosystems, USA). The relative primers involved in the experiments are listed in **Table 1**. β -
206 Actin was considered an internal control to normalize the expression levels of genes. The cDNA
207 was denatured at 95°C for 10 min followed by 40 cycles of PCR (95°C for 15 s, 60°C for 60 s).

208

209 **Statistical analysis**

210

211 Data were analyzed using SPSS 18.0, and the results were presented as mean \pm SEM.
212 Differences were considered significant if $P < 0.05$. Statistical analysis included one-way
213 analysis of variance, the Student's t-test, the Kruskal - Wallis H Test, and repeated measures
214 analysis of variance.

215

216 **RESULTS**

217

218 **LC - HRMS detection of the main chemical constituents**

219

220 We performed the LC - HRMS assay to characterize the constituents in the extract. Ten
221 compounds were putatively identified in the extract according to a previous report (*Chen et al.*,
222 *2010*). We detected some β -carboline alkaloids, such as stellarine A - C, dichotomine B, H, and
223 L, glucodichotomine B as well as vanillin, 5-hydroxymethylfurfural (Fig. 1 and Table 2).

224

225 **RSE inhibited body weight gain in C57BL/6 mice induced by high-fat diet**

226

227 To investigate the effect of RSE on body weight gain, we selected the most widely used inbred
228 strain C57BL/6 mouse, which is susceptible to diet-induced obesity, type 2 diabetes and
229 atherosclerosis (*Sun et al.*, *2016*; *Xia et al.*, *2016*). The dose of RSE was determined by using a
230 series of complex mathematical operation according to the dose of humans (15 g natural plant
231 medicine/60 kg body weight/day) and pharmacology of traditional Chinese medicine (*Zhang*,
232 *2002*). The C57BL/6 mice were fed on a chow diet, HF diet or HF diet supplemented with 1%
233 RSE for 8 weeks. The data revealed that the average body weight in the HF group was
234 significantly higher than that of the Chow group (Fig. 2A), whereas the body weight of the HF +
235 RSE group was evidently lower than that in the HF group from Week 2 to Week 8 (Fig. 2A). The
236 data indicated that RSE could inhibit body weight gain induced by HF-diet in mice. There was
237 no significant difference of food intake between the HF and HF + RSE groups (Fig. 2B).
238 Furthermore, we observed the weekly food intake of the mice. The weekly intake of the three
239 groups remained in a state of equilibrium (Fig. 2C). Thus, the lower body weight in RSE-treated
240 mice was not caused by a lower calorie intake.

241

242 Next, we measured the adipocyte size using the H & E stain. The results revealed that the size

243 of WAT in the HF group was considerably larger than that of the Chow group, and RSE
244 treatment reduced the size of WAT in HF + RSE group (Fig. 2D-2E). The data supported the
245 conclusion that RSE inhibits body weight gain.

246

247 Inhibition of lipid absorption in the intestine or increase of energy expenditure may result in
248 weight reduction. To test whether RSE affected the lipid absorption and energy expenditure, we
249 determined the total cholesterol and triglyceride content of the feces of the mice, and measured
250 rectal temperature. The RSE-treated mice did not exhibit an increase in the TC and TG content
251 of feces (Fig. 2F-2G); however, the body temperature of the RSE-treated mice was notably
252 higher than that of the mice in the other groups (Fig. 2H). Hence, an increase in energy
253 consumption, and not the inhibition of intestinal lipid absorption, may be responsible for the
254 reduction in body weight in HF + RSE group mice.

255

256 **RSE reduced fasting blood glucose and ameliorated insulin tolerance in high-fat diet-**
257 **induced obese C57BL/6 mice at 15 and 30 min**

258

259 Obesity is a cause for insulin resistance and type II diabetes. Therefore, we measured the fasting
260 blood glucose levels and glucose tolerance in the mice (Fig. 3A). RSE- treated mice exhibited
261 lower fasting glucose levels than did the HF-fed mice (Fig. 3B). However, the blood glucose
262 levels did not change following intraperitoneal injection of glucose. Then we tested the insulin
263 tolerance in the mice. The results revealed that the blood glucose levels of the HF + RSE group
264 were lowered than those of the HF group at 15, and 30 min (Fig. 3C).

265

266 **RSE lowered the lipid profile in serum and liver**

267

268 Obesity may be accompanied by hyperlipidemia. Therefore, we measured the lipid levels in
269 serum and liver tissue. The fasting serum TG, TC, and LDL-c levels of the HF + RSE group
270 were slightly lower than those of the HF group, although the levels were not significantly
271 different between both groups (Fig. 4A). Similarly, the hepatic TG and TC levels were also
272 lower in the RSE-treated mice (Fig. 4B). Then, we tested the serum levels of ALT and AST, the
273 two indicators of liver damage. The levels of ALT of the HF group were evidently higher than
274 those of the Chow diet-fed mice, indicating potential damage to liver function. RSE treatment,
275 however, did not change the ALT and AST concentrations in HF group mice (Fig. 4C-4D).

276

277 **RSE induced the expression of metabolic gene *in vivo***

278 The genes for uncoupling proteins (UCPs), namely UCP1, UCP2, and UCP3, are closely related
279 to energy metabolism. In view of the rise of body temperature, we tested the expression of these
280 genes in BAT, which participates in energy consumption and heat production. The expression of
281 the genes in the RSE-treated mice BAT was not notably different from that of the HF-fed mice
282 (Fig. 5A). White beige fat, indicated by high UCP1 expression (*Nedergaard & Cannon, 2014*),
283 which increases energy metabolism, may also be a mechanism of fat reduction. Therefore, we

284 analyzed the expression of UCPs in the WAT. The data revealed that the mRNA of UCP1 and
285 UCP3 increased markedly, suggesting the induction of WAT browning by RSE (Fig. 5B).

286

287 PPARs are the ligand-activated nuclear transcription factors regulating the gene expression of
288 glucose and lipid metabolism. A reporter assay was performed to test whether the RSE alters
289 transactivities of PPAR α , β , γ . The results showed that RSE did not change the transcription
290 activity of PPARs, suggesting that RSE does not activate PPARs directly.

291 We examined the mRNA expression levels of PPARs and their target genes in the WAT. RSE
292 clearly increased the mRNA expression of PPARs and acetyl coenzyme A carboxylase (ACC),
293 acyl-CoA oxidase (ACO), adipose fatty acid-binding protein (aP2), cluster of differentiation 36
294 (CD36), peroxisome proliferator-activated receptor coactivator-1 α and -1 β (PGC-1 α and PGC-
295 1 β), glucose transporter 4 (GLUT 4) as well as UCP1, and UCP3. Among them, PPAR β , PPAR γ ,
296 UCP1, UCP3, ACO, aP2, and CD 36 were significant (Fig. 5B). Taken together, the data
297 suggested that RSE may regulate body weight and blood glucose levels through the enhancement
298 of PPAR signaling.

299

300 DISCUSSION

301

302 MS is a complex health problem involving several complications and is prevalent in both
303 developed and developing countries. Host genetic and environmental factors can result in MS
304 (*Lim et al., 2016*). Wu et al. reported that physical activity can serve as an effective means to
305 prevent metabolic syndrome (*Wu et al., 2016*). However, physical activity alone does not
306 effectively prevent MS; drugs are also required. Therefore, the development of new drugs to
307 manage MS is necessary.

308

309 RS, a common Chinese herbal medicine, has been used in the treatment of deficiency-heat
310 syndrome. Some compounds extracted from RS have different potential pharmacological effects,
311 for instance, saikosaponin C can prevent Alzheimer's disease in various neuronal models and
312 saikosaponin D can inhibit selectin-mediated cell adhesion (*Jang et al., 2014*). Furthermore, the
313 plant extract of RS is used as a reducing agent to convert gold ions to gold nanoparticles in a
314 biofabrication process. An increasing number applications of RS have been recently discovered,
315 such as prevention of depression and anxiety-like behaviors in rats exposed to repeated restraint
316 stress. However, there was no reported that RS could treat obesity. We should investigated
317 promising new features of Chinese traditional medicine.

318

319 Through LC-HRMS, we detected some chemical constituents of RSE that were mainly β -
320 carboline alkaloids (β CAs): dichotomine B, dichotomine H, dichotomine L, stellarine A-C and
321 glucodichotomine B. β CAs are a type of heterocyclic amines; they are considered to be products
322 of cooking meat (*Lavita et al., 2015*), and widely distributed in the nature and their action is
323 similar to that of indole alkaloids. Recent years, cyclopeptides have received considerable
324 attention from pharmacologists, chemists and biochemists owing to their various bioactivities

325 such as antiviral, antineoplastic, immunomodulate properties. For example, as a main chemical
326 constituent of *Psammosilene tunicoides*, stallarine A, a new cyclic heptapeptide (Zhao *et al.*,
327 1995) showed the bacteriostatic activity to a certain extent (Wang *et al.*, 2012). Besides, a study
328 reported that glucodichotomine B and neolignan glycosides isolated from the root of RS showed
329 antiallergic activities (Morikawa *et al.*, 2004). In a word, β CAs exhibit anti-tumor, anti-microbial,
330 anti-viral (Li *et al.*, 2006), anti-oxidative (Hadjaz *et al.*, 2011) and insecticidal activities.
331 Moreover, according to some previous studies, we found that many alkaloids were identified to
332 have PPARs agonistic activity: picrasidine C and picrasidine N (Zhao *et al.*, 2016), isolated from
333 the root of *Picrasma quassioides*, were identified to have PPAR α and PPAR β agonistic activity
334 respectively (Zhao *et al.*, 2016); evodiamine, an indole alkaloid extracted from the Chinese
335 medicine *evodia*, has been shown to inhibit tumor cell invasion and protect the cardiovascular
336 system through activating PPAR γ (Ge *et al.*, 2015). In the present study, β CAs constituted a
337 large proportion of the RSE; therefore, we suspect that they played a role in treating obesity
338 through regulating PPARs.

339

340 In the present study, RSE treatment significantly reduced body weight and WAT size in the
341 C57BL/6 mice compared with HF group. Weight-reduction therapy involves three major
342 methods: reducing food intake, increasing energy expenditure, and inhibiting lipid absorption.
343 We did not observe significant changes in food consumption and lipid absorption in the intestine.
344 Interestingly, the rectal temperature of RSE-treated mice was markedly higher than that of HF-
345 diet-fed mice. These data suggest that RSE could block body-weight gain by increasing the
346 energy metabolism rather than by reducing calorie intake or inhibition of intestinal lipid
347 absorption. Our findings indicated that RS also could be used to increase the body temperature in
348 obese subjects.

349

350 RSE-treated mice exhibited lower fasting blood glucose levels and improved insulin tolerance
351 than the mice in the other groups. Obesity is a crucial risk factor for metabolic disorders,
352 moreover, weight reduction may improve insulin tolerance and diabetes. Therefore, the body-
353 weight reduction might contributed to the glucose-lowering effects of RSE.

354

355 For the mechanism of increasing energy expenditure, we focused on the mRNA expression
356 levels of related genes in BAT and WAT, which play a vital role in energy metabolism. Recently,
357 “beige adipocytes” have been identified (Wu *et al.*, 2012), which share common morphology and
358 function with classical BAT, but they are observed in WAT (Shin *et al.*, 2016). Beige adipocytes
359 can promote browning in WAT and increase the expression levels of UCPs, and efficiently
360 increasing energy expenditure by elevating thermogenesis. Therefore, “beige adipocytes”
361 provide a platform for anti-obesity therapy (Harms & Seale, 2013; Pfeifer & Hoffmann, 2015).
362 Our results suggested that RSE might block body weight gain induced by HF-diet in C57BL/6
363 mice through the elevation of energy metabolism genes expression promoting the white fat beige,
364 evidenced by the high-level expression of UCPs (Nedergaard & Cannon, 2014).

365

366 According to the experimental results, the expression of PPARs and downstream genes were
367 increased, indicating that RSE may activate PPARs signaling. Uncoupling protein3 (UCP3) is a
368 mitochondrial anion carrier protein, regarded as an obesity candidate gene. It is mainly
369 distributed in the skeletal muscles and BAT, and it is also expressed in WAT. UCP3 could
370 mediate the oxidation process and ADP uncoupling phosphorylation process, thereby preventing
371 energy storage in the form of ATP but releasing it in the form of heat. Evidence supported the
372 role of UCP3 in the lipid metabolic, glucose metabolic(Busiello, Savarese & Lombardi, 2015),
373 and energy balance of the body, specifically glucose oxidation and insulin sensitivity(Bezaire,
374 Seifert & Harper, 2007; Busiello, Savarese & Lombardi, 2015). RSE sharply increased the
375 mRNA levels of PPARs and target gene UCP3, thereby suggesting that RS prevents HF-diet-
376 induced obesity in C57BL/6 mice mainly through the activation of PPARs and UCP3 signaling.

377

378 CONCLUSION

379

380 RS may alleviate metabolic disorders, by inhibiting body weight increase, reducing fasting blood
381 glucose levels, and ameliorating insulin tolerance in HF diet-induced obese C57BL/6 mice
382 through the increase of UCP3 and PPARs. Our data suggest that RS may be used to prevent
383 metabolic disorders in addition to its traditional uses. However, the potential effects of RS have
384 yet to be discovered, and the identification of active ingredients and elucidation of mechanisms
385 underlying the alleviation of metabolic disorders call for further inquiry.

386

387 ACKNOWLEDGMENTS

388

389 The authors would like to thank F. Li (State Key Laboratory of Natural Medicines, Department
390 of Natural Medicinal Chemistry, China Pharmaceutical University, People's Republic of China)
391 for his useful suggestions and revision.

392

393 REFERENCES

394 **Morikawa T, Sun B, Matsuda H, Wu LJ, Harima S, Yoshikawa M. 2004.** Bioactive constituents from Chinese natural
395 medicines. XIV. New glycosides of beta-carboline-type alkaloid, neolignan, and phenylpropanoid from
396 *Stellaria dichotoma* L. var. *lanceolata* and their antiallergic activities. *Chem Pharm Bull (Tokyo)*
397 **52(10):1194-1199.**

398 **Eckel RH, Alberti KG, Grundy SM, Zimmet PZ. 2010.** The metabolic syndrome. *Lancet* **375(9710):181-183.**

399 **Ginsberg HN. 2003.** Treatment for patients with the metabolic syndrome. *Am J Cardiol* **91(7A):29E-39E.**

400 **Apovian CM, Aronne LJ, Bessesen DH, McDonnell ME, Murad MH, Pagotto U, Ryan DH, Still CD. 2015.**
401 Pharmacological management of obesity: an endocrine Society clinical practice guideline. *J Clin Endocrinol*
402 **Metab** **100(2):342-362.**

403 **Harms M, Seale P. 2013.** Brown and beige fat: development, function and therapeutic potential. *Nat Med*
404 **19(10):1252-1263.**

405 **Izzi-Engbeaya C, Salem V, Atkar RS, Dhillon WS. 2015.** Insights into Brown Adipose Tissue Physiology as Revealed by

- 406 Imaging Studies. *Adipocyte* **4(1)**:1-12.
- 407 **Kim SH, Plutzky J. 2016.** Brown Fat and Browning for the Treatment of Obesity and Related Metabolic Disorders.
408 *Diabetes Metab J* **40(1)**:12-21.
- 409 **Francis GA, Fayard E, Picard F, Auwerx J. 2003.** Nuclear receptors and the control of metabolism. *Annu Rev*
410 *Physiol* **65**(261-311).
- 411 **Desvergne B, Wahli W. 1999.** Peroxisome proliferator-activated receptors: nuclear control of metabolism. *Endocr*
412 *Rev* **20(5)**:649-688.
- 413 **Wahli W, Braissant O, Desvergne B. 1995.** Peroxisome proliferator activated receptors: transcriptional regulators
414 of adipogenesis, lipid metabolism and more. *Chem Biol* **2(5)**:261-266.
- 415 **Jia Y, Qi C, Zhang Z, Hashimoto T, Rao MS, Huyghe S, Suzuki Y, Van Veldhoven PP, Baes M, Reddy JK. 2003.**
416 Overexpression of peroxisome proliferator-activated receptor-alpha (PPARalpha)-regulated genes in liver
417 in the absence of peroxisome proliferation in mice deficient in both L- and D-forms of enoyl-CoA
418 hydratase/dehydrogenase enzymes of peroxisomal beta-oxidation system. *J Biol Chem* **278(47)**:47232-
419 47239.
- 420 **Barger PM, Kelly DP. 2000.** PPAR signaling in the control of cardiac energy metabolism. *Trends Cardiovasc Med*
421 **10(6)**:238-245.
- 422 **Gilde AJ, Van Bilsen M. 2003.** Peroxisome proliferator-activated receptors (PPARS): regulators of gene expression
423 in heart and skeletal muscle. *Acta Physiol Scand* **178(4)**:425-434.
- 424 **Bishop-Bailey D. 2000.** Peroxisome proliferator-activated receptors in the cardiovascular system. *Br J Pharmacol*
425 **129(5)**:823-834.
- 426 **Puddu P, Puddu GM, Muscari A. 2003.** Peroxisome proliferator-activated receptors: are they involved in
427 atherosclerosis progression? *Int J Cardiol* **90(2-3)**:133-140.
- 428 **Thompson EA. 2007.** PPARgamma physiology and pathology in gastrointestinal epithelial cells. *Mol Cells* **24(2)**:167-
429 176.
- 430 **Spiegelman BM. 1998.** PPAR-gamma: adipogenic regulator and thiazolidinedione receptor. *Diabetes* **47(4)**:507-514.
- 431 **Barroso I, Gurnell M, Crowley VE, Agostini M, Schwabe JW, Soos MA, Maslen GL, Williams TD, Lewis H, Schaffer**
432 **AJ, Chatterjee VK, O'Rahilly S. 1999.** Dominant negative mutations in human PPARgamma associated with
433 severe insulin resistance, diabetes mellitus and hypertension. *Nature* **402(6764)**:880-883.
- 434 **Chen YF, Kuo PC, Chan HH, Kuo IJ, Lin FW, Su CR, Yang ML, Li DT, Wu TS. 2010.** beta-carboline alkaloids from
435 *Stellaria dichotoma* var. lanceolata and their anti-inflammatory activity. *J Nat Prod* **73(12)**:1993-1998.
- 436 **Cao LH, Zhang W, Luo JG, Kong LY. 2012.** Five New β -Carboline-Type Alkaloids from *Stellaria dichotoma* var.
437 lanceolata. *ChemInform* **43(40)**:
- 438 **Teng J. 1985.** [Research on the originol plant *Stellaria dichotoma* var. Lanceolata in the ben-cao pharmaopeia].
439 *Zhong Yao Tong Bao* **10(4)**:15-16.
- 440 **Sun B, Morikawa T, Matsuda H, Tewtrakul S, Wu LJ, Harima S, Yoshikawa M. 2004.** Structures of new beta-
441 carboline-type alkaloids with antiallergic effects from *Stellaria dichotoma*(1,2). *J Nat Prod* **67(9)**:1464-
442 1469.
- 443 **Morita H, Iizuka T, Choo CY, Chan KL, Itokawa H, Takeya K. 2005.** Dichotomins J and K, vasodilator cyclic peptides
444 from *Stellaria dichotoma*. *J Nat Prod* **68(11)**:1686-1688.
- 445 **Sun H, Wang X, Chen J, Song K, Gusdon AM, Li L, Bu L, Qu S. 2016.** Melatonin improves non-alcoholic fatty liver
446 disease via MAPK-JNK/P38 signaling in high-fat-diet-induced obese mice. *Lipids Health Dis* **15(1)**:202.

- 447 Xia SF, Le GW, Wang P, Qiu YY, Jiang YY, Tang X. 2016. Regressive Effect of Myricetin on Hepatic Steatosis in Mice
448 Fed a High-Fat Diet. *Nutrients* **8**(12):
- 449 Zhang, DF. 2002. Experiments of pharmacology and traditional Chinese medicine pharmacology . *Shanghai:*
450 *Shanghai Scientific and Technical Publishers, 8.*
- 451 Nedergaard J, Cannon B. 2014. The browning of white adipose tissue: some burning issues. *Cell Metab* **20**(3):396-
452 407.
- 453 Lim MY, You HJ, Yoon HS, Kwon B, Lee JY, Lee S, Song YM, Lee K, Sung J, Ko G. 2016. The effect of heritability and
454 host genetics on the gut microbiota and metabolic syndrome. *Gut*
- 455 Wu S, Fisher-Hoch SP, Reininger B, McCormick JB. 2016. Recommended Levels of Physical Activity Are Associated
456 with Reduced Risk of the Metabolic Syndrome in Mexican-Americans. *PLoS One* **11**(4):e0152896.
- 457 Jang MJ, Kim YS, Bae EY, Oh TS, Choi HJ, Lee JH, Oh HM, Lee SW. 2014. Saikosaponin D isolated from Bupleurum
458 falcatum inhibits selectin-mediated cell adhesion. *Molecules* **19**(12):20340-20349.
- 459 Lavita SI, Aro R, Kiss B, Manto M, Duez P. 2015. The Role of beta-Carboline Alkaloids in the Pathogenesis of
460 Essential Tremor. *Cerebellum*
- 461 Zhao YR, Zhou J, Wang XK, Huang XL, Wu HM, Zou C. 1995. Cyclopeptides from *Stellaria yunnanensis*.
462 *Phytochemistry* **40**(5):1453-1456.
- 463 Wang L, Gong XJ, Zhou X, Xian C, Yang SL, Yang ZN. 2012. [Chemical constituents of *Psammosilene tunicoides* and
464 bacteriostatic activity]. *Zhongguo Zhong Yao Za Zhi* **37**(23):3577-3580.
- 465 Li XL, Cheng X, Yang LM, Wang RR, Zheng YT, Xiao WL, Zhao Y, Xu G, Lu Y, Chang Y, Zheng QT, Zhao QS, Sun HD.
466 2006. Dichotomains A and B: two new highly oxygenated phenolic derivatives from *Dicranopteris*
467 *dichotoma*. *Org Lett* **8**(9):1937-1940.
- 468 Hadjaz F, Besret S, Martin-Nizard F, Yous S, Dilly S, Lebegue N, Chavatte P, Duriez P, Berthelot P, Carato P. 2011.
469 Antioxydant activity of beta-carboline derivatives in the LDL oxidation model. *Eur J Med Chem* **46**(6):2575-
470 2585.
- 471 Zhao S, Kanno Y, Li W, Wakatabi H, Sasaki T, Koike K, Nemoto K, Li H. 2016. Picrasidine N Is a Subtype-Selective
472 PPARbeta/delta Agonist. *J Nat Prod* **79**(4):879-885.
- 473 Zhao S, Kanno Y, Li W, Sasaki T, Zhang X, Wang J, Cheng M, Koike K, Nemoto K, Li H. 2016. Identification of
474 Picrasidine C as a Subtype-Selective PPARalpha Agonist. *J Nat Prod* **79**(12):3127-3133.
- 475 Ge X, Chen S, Liu M, Liang T, Liu C. 2015. Evodiamine Attenuates PDGF-BB-Induced Migration of Rat Vascular
476 Smooth Muscle Cells through Activating PPARgamma. *Int J Mol Sci* **16**(12):28180-28193.
- 477 Wu J, Bostrom P, Sparks LM, Ye L, Choi JH, Giang AH, Khandekar M, Virtanen KA, Nuutila P, Schaart G, Huang K,
478 Tu H, van Marken Lichtenbelt WD, Hoeks J, Enerback S, Schrauwen P, Spiegelman BM. 2012. Beige
479 adipocytes are a distinct type of thermogenic fat cell in mouse and human. *Cell* **150**(2):366-376.
- 480 Shin JH, Lee SH, Kim YN, Kim IY, Kim YJ, Kyeong DS, Lim HJ, Cho SY, Choi J, Wi YJ, Choi JH, Yoon YS, Bae YS, Seong
481 JK. 2016. AHNAK deficiency promotes browning and lipolysis in mice via increased responsiveness to beta-
482 adrenergic signalling. *Sci Rep* **6**(23426).
- 483 Pfeifer A, Hoffmann LS. 2015. Brown, beige, and white: the new color code of fat and its pharmacological
484 implications. *Annu Rev Pharmacol Toxicol* **55**(207-227).
- 485 Busiello RA, Savarese S, Lombardi A. 2015. Mitochondrial uncoupling proteins and energy metabolism. *Front*
486 *Physiol* **6**(36).
- 487 Bezaire V, Seifert EL, Harper ME. 2007. Uncoupling protein-3: clues in an ongoing mitochondrial mystery. *FASEB J*

488 **21(2):312-324.**

489

490

491

492

493

494

495

496

497

498

499

500

501

502

503

504

505

506

507

508

509

510

511

512

513

514

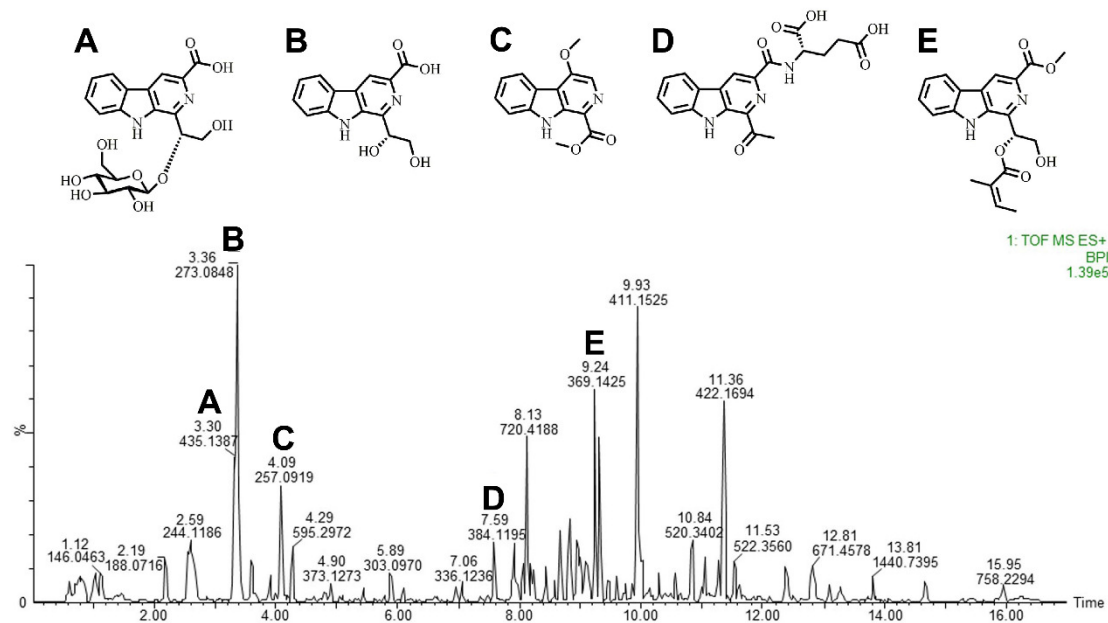
515

516

517

518

519 **Fig 1**



520

521

522 **Carbolines of RSE identified through liquid chromatography-high resolution mass**
 523 **spectrometry.** Total ion chromatogram of the chemical composition in RSE identified through
 524 LC-HRMS, performed using positive ions channel. (A) Glucodichotomine B (B) Dichotomine B
 525 (C) β -carboline alkaloid (D) Dichotomine H (E) Dichotomine L

526

527

528

529

530

531

532

533

534

535

536

537

538

539

540

541

542

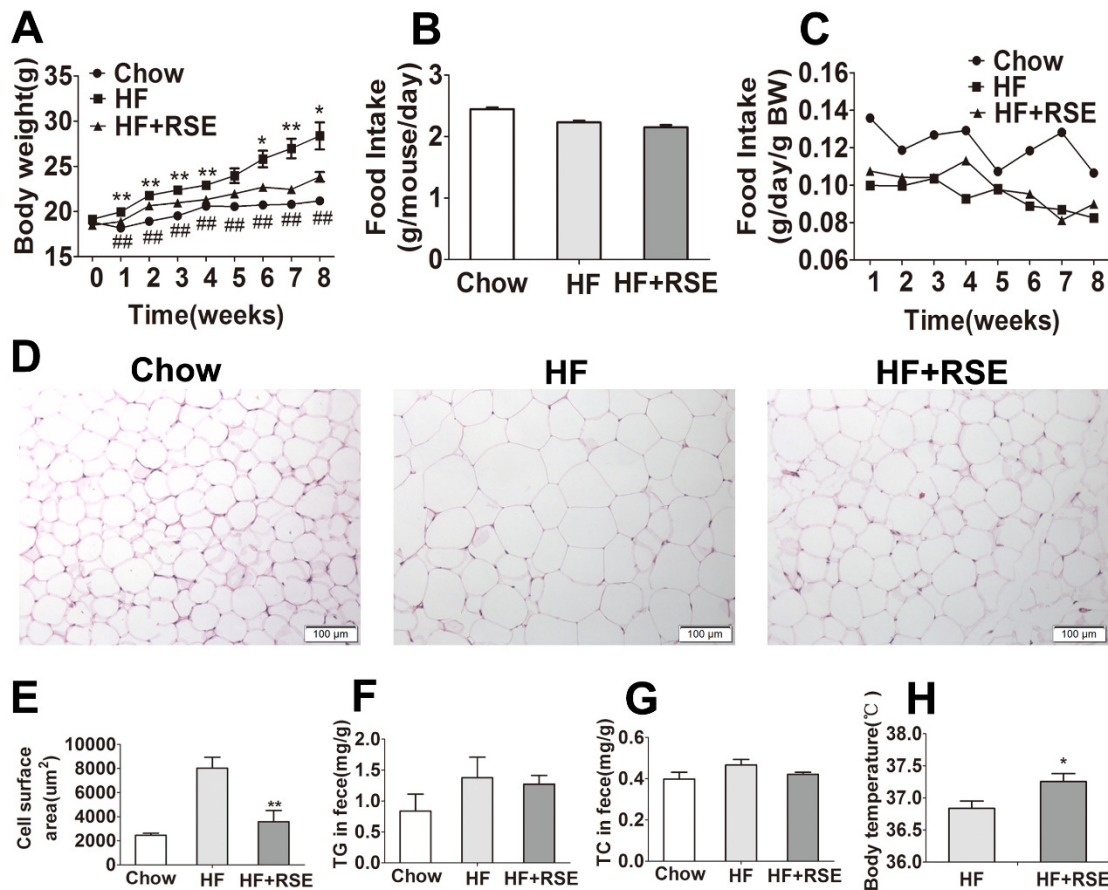
543

544

545

546

547 Fig 2



548

549 **RSE prevents metabolic disorders in high-fat-diet-induced obese C57BL/6 mice.** The mice
 550 were fed with Chow, HF-diet, and HF-diet mixed with 1% (w/w) RSE for 8 weeks. (A) Body
 551 weight (B) Food intake amount (C) Food intake dynamic figure (D) H&E staining of WAT
 552 sections (200 ×) (E) Cell surface area of WAT (F) Feces TG levels (G) Feces TC levels (H)
 553 Body temperature. Data are presented as mean ± SEM (Chow: n = 10; others: n = 8). * $P < 0.05$,
 554 ** $P < 0.01$ vs the HF group. # $P < 0.05$, ## $P < 0.01$ were the Chow vs the HF group.

555

556

557

558

559

560

561

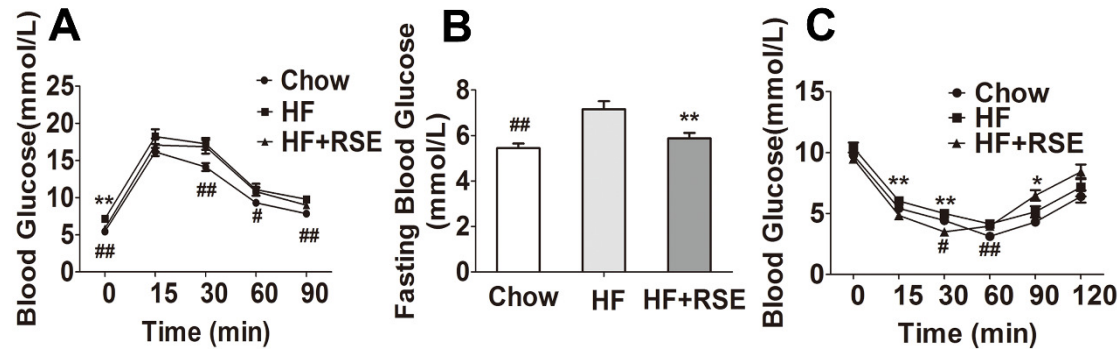
562

563

564

565
566
567
568

Fig 3



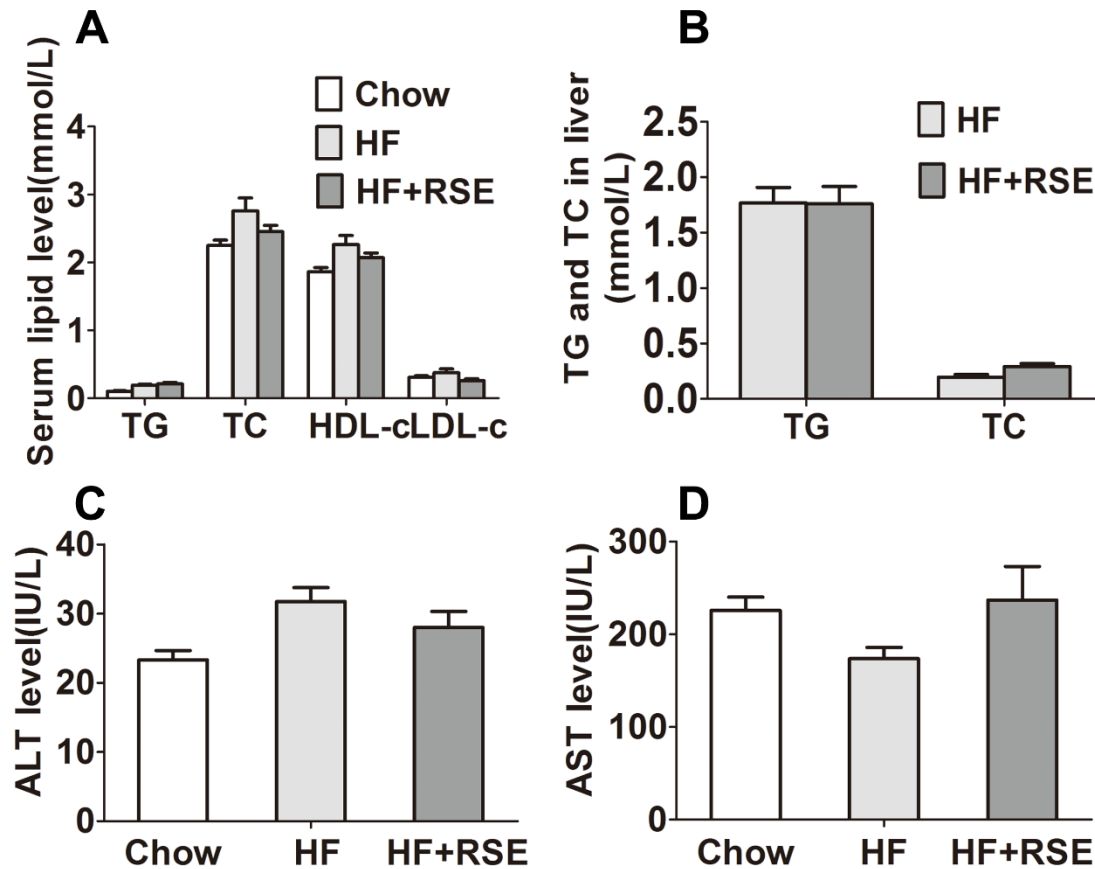
569

570 **RSE improves glucose metabolism and insulin tolerance in high-fat-diet-induced C57BL/6**
571 **mice.** (A) Intraperitoneal glucose tolerance test at 0, 15, 30, 60, and 90 min. The mice were
572 fasted for 12 h before measuring blood glucose levels at 0 min (B) Fasting glucose levels (C)
573 Intraperitoneal insulin tolerance test at 0, 15, 30, 60, 90, and 120 min. The mice were not fasted.
574 Data are presented as mean \pm SEM (Chow: n = 10; others: n = 8). * $P < 0.05$, ** $P < 0.01$ vs the
575 HF group. # $P < 0.05$, ## $P < 0.01$ were the Chow vs the HF group.

576
577
578
579
580
581
582
583
584
585
586
587
588
589
590
591
592
593
594
595
596

597
598
599
600
601
602

Fig 4



603

604 **Effects of RSE on serum and liver lipid levels in high-fat-diet-induced C57BL/6 mice.** (A)
605 Serum TC, TG, HDL-c, LDL-c levels (B) Liver TG and TC levels (C) ALT levels in serum (D)
606 AST levels in serum. Data are presented as mean \pm SEM (Chow: n = 10; others: n = 8), Figure B
607 comparison between group pairs were K-W H test because of the data not following normal
608 distribution. * $P < 0.05$, ** $P < 0.01$ vs the HF group.

609

610

611

612

613

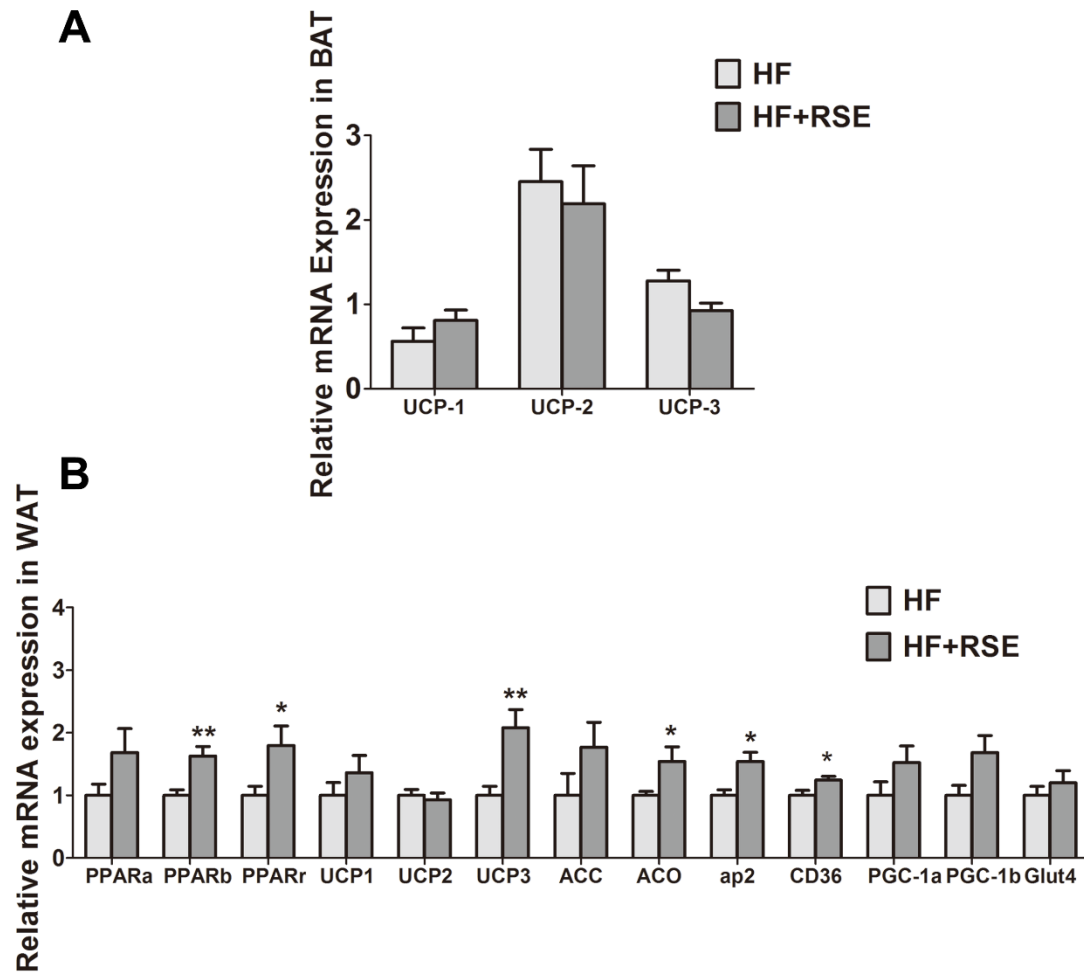
614

615

616

617
618
619
620
621
622
623
624

Fig 5



625
626
627
628
629
630
631
632
633
634

RSE induced the expression of UCPs, PPARs and their target genes. (A) Relative expression levels of UCPs in the brown adipose tissue (B) Relative expression levels of UCPs and PPARs target genes in the white adipose tissue. β -actin was used as an internal control for modifying the mRNA level. Data are presented as mean \pm SEM (Chow: n = 10; others: n = 8). * $P < 0.05$, ** $P < 0.01$ vs the HF group.

635
636
637
638
639
640
641
642
643
644

645 Table 1: Sequences of the primers used in real-time PCR of mouse tissue.

Gene	Forward primer	Reverse primer
β -Actin	TGTCCACCTTCCAGCAGATGT	AGCTCAGTAACAGTCCGCCTAGA
PPAR α	AGGCTGTAAGGGCTTCTTTC	GGCATTGTGTTCCGGTTCTTC
	G	
PPAR β	AGTGACCTGGCGCTCTTCAT	CGCAGAATGGTGTCTGGAT
PPAR γ	CGCTGATGCACTGCCTATGA	AGAGGTCCACAGAGCTGATTCC
PGC-1 α	TGTTCCCGATCACCATATTCC	GGTGTCTGTAGTGGCTTGATTCC
PGC-1 β	GGGTGCGCCTCCAAGTG	TCTACAGACAGAAGATGTTATGT
		GAACAC
aP2	CATGGCCAAGCCCAACAT	CGCCCAGTTTGAAGGAAATC
ACC	GAATCTCCTGGTGACAATGC	GGTCTTGCTGAGTTGGGTTAGCT
	TTATT	
ACO	CAGCACTGGTCTCCGTCATG	CTCCGGACTACCATCCAAGATG
UCP1	CATCACCACCCTGGCAAAA	AGCTGATTTGCCTCTGAATGC
UCP2	GGGCACTGCAAGCATGTGTA	TCAGATTCCTGGGCAAGTCACT

UCP3 TGGCCCAACATCACAAGAAA TCCAGCAACTTCTCCTTGATGA

CD36 GCTTGCAACTGTCAGCACAT GCCTTGCTGTAGCCAAGAAC

Glut4 GTAACTTCATTGTCGGCATG AGCTGAGATCTGGTCAAACG

G

646

647

648

649

650

651

652

653

654

655 Table 2: Chemical constituents of RSE identified through liquid chromatography-high resolution mass
656 spectrometry.

Peak	Rt(min)	MS-Mol. wt.+H	Actual Mol. wt.+H	Formula	Constituents
1	3.30	435.1387	435.1359	C ₂₀ H ₂₂ N ₂ O ₉	Glucodichotomine B
2	3.362	273.0850	273.0875	C ₁₄ H ₁₂ N ₂ O ₄	Dichotomine B
3	4.070	257.0919	257.0926	C ₁₄ H ₁₂ N ₂ O ₃	β-carboline alkaloid
4	7.59	384.1195	384.1151	C ₁₉ H ₁₇ N ₃ O ₆	Dichotomine H
5	9.238	369.1425	369.1450	C ₂₀ H ₂₀ N ₂ O ₅	Dichotomine L
6	7.614	254.0919	254.0930	C ₁₄ H ₁₁ N ₃ O ₂	Stellarine A
7	8.190	338.1138	338.1141	C ₁₈ H ₁₅ N ₃ O ₄	Stellarine B
8	8.940	269.0920	269.0926	C ₁₅ H ₁₂ N ₂ O ₃	Stellarine C
9	3.793	153.0562	153.0552	C ₈ H ₈ O ₃	Vanillin
10	2.058	127.0392	127.0395	C ₆ H ₆ O ₃	5-Hydroxymethylfurfural

657 Rt: retention time (min), MS-Mol. wt.+H: primary mass spectrometry, Actual Mol. wt.+H: actual molecular
658 weight.

659

660